

Cite this: *Chem. Sci.*, 2022, 13, 1390

All publication charges for this article have been paid for by the Royal Society of Chemistry

Received 14th October 2021  
Accepted 26th December 2021

DOI: 10.1039/d1sc05651d

rsc.li/chemical-science

# Nickel/Brønsted acid dual-catalyzed regio- and enantioselective hydrophosphinylation of 1,3-dienes: access to chiral allylic phosphine oxides†

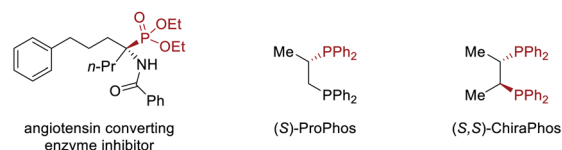
Jiao Long,<sup>a</sup> Yuqiang Li,<sup>a</sup> Weining Zhao<sup>\*b</sup> and Guoyin Yin<sup>ID</sup><sup>\*a</sup>

While chiral allylic organophosphorus compounds are widely utilized in asymmetric catalysis and for accessing bioactive molecules, their synthetic methods are still very limited. We report the development of asymmetric nickel/Brønsted acid dual-catalyzed hydrophosphinylation of 1,3-dienes with phosphine oxides. This reaction is characterized by an inexpensive chiral catalyst, broad substrate scope, and high regio- and enantioselectivity. This study allows the construction of chiral allylic phosphine oxides in a highly economic and efficient manner. Preliminary mechanistic investigations suggest that the 1,3-diene insertion into the chiral Ni–H species is a highly regioselective process and the formation of the chiral C–P bond is an irreversible step.

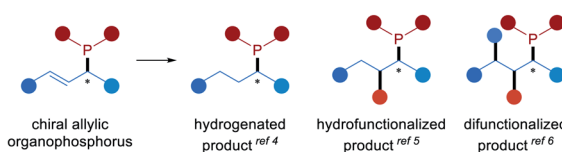
## Introduction

Chiral organophosphorus compounds are widely utilized as synthetic building blocks for accessing bioactive molecules and functional materials.<sup>1</sup> Indeed, as chiral ligands, they also play significant roles in transition metal-catalyzed<sup>2</sup> and organocatalytic<sup>2h,3</sup> asymmetric transformations (Fig. 1a). Chiral allylic organophosphorus compounds contain pendant unsaturation that might be leveraged for downstream synthesis applications. For instance, they could undergo hydrogenation,<sup>4</sup> hydrofunctionalization<sup>5</sup> or difunctionalization<sup>6</sup> to deliver a series of structurally diverse chiral phosphines (Fig. 1b). Despite the versatility of chiral allylic organophosphorus compounds, efficient methods for their preparation are rather limited.<sup>7</sup> Asymmetric allylic substitution of P–H with electrophiles containing a good leaving group was an efficient strategy to deliver chiral allylic organophosphorus compounds (Fig. 1c, left),<sup>7b,8</sup> wherein P-stereogenic organophosphorus compounds are usually obtained.<sup>8</sup> Recently, the enantioselective hydrofunctionalization of conjugated 1,3-dienes, allenes and alkynes with C-,<sup>9</sup> N-,<sup>10</sup> or S-nucleophiles<sup>11</sup> has attracted broad attention and has been developed as a powerful tool to synthesize chiral allylic compounds.<sup>12</sup> Asymmetric hydrophosphination (including hydrophosphonylation and hydrophosphinylation)<sup>13</sup> of 1,3-dienes with P–H nucleophiles is undoubtedly a straightforward and

### (a) Representative bioactive molecules and ligands bearing a chiral phosphine

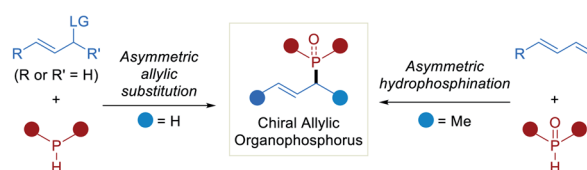


### (b) Applications of chiral allylic organophosphorus compounds

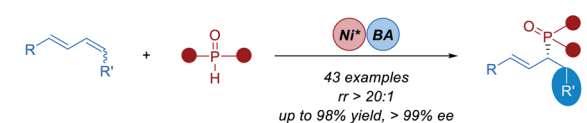


chiral ally organophosphorus as a platform to access structurally diverse chiral phosphine

### (c) Enantioselective synthesis of chiral allylic organophosphorus compounds



### (d) Nickel/BA-catalyzed asymmetric hydrophosphinylation of 1,3-dienes (this work)



- ◆ Inexpensive metal and chiral ligand
- ◆ Excellent regio- and enantioselectivity
- ◆ Broad substrate scope
- ◆ Mechanistic investigations

<sup>a</sup>The Institute for Advanced Studies, Wuhan University, Wuhan 430072, China. E-mail: yinguoyin@whu.edu.cn<sup>b</sup>College of Pharmacy, Shenzhen Technology University, Shenzhen 518118, China. E-mail: zhaoweining@sztu.edu.cn

† Electronic supplementary information (ESI) available: For experimental details and characterization data, see DOI: 10.1039/d1sc05651d

Fig. 1 (a) Representative bioactive molecules and ligands bearing a chiral phosphine; (b) applications of chiral allylic organophosphorus compounds; (c) enantioselective synthesis of chiral allylic organophosphorus compounds; (d) nickel/BA-catalyzed asymmetric hydrophosphinylation of 1,3-dienes (this work).

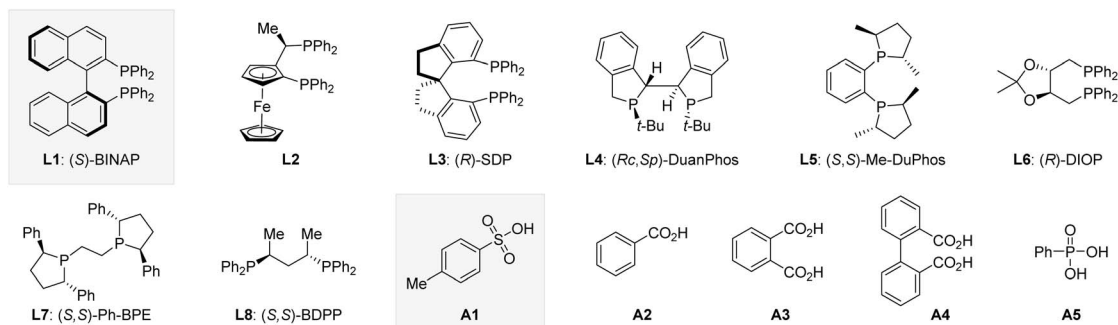


atom-efficient approach to construct chiral allylic organophosphorus compounds. A seminal study of enantioselective coupling of terminal 1,3-dienes and phosphine oxides affording a series of chiral  $\alpha$ -methyl allylic phosphine oxides by palladium catalysis was demonstrated by Dong and coworkers in 2018 (Fig. 1c, right).<sup>14</sup> When we were preparing this manuscript, an elegant example of Pd-catalyzed hydrophosphinylation of allenes with phosphine oxides producing chiral allylic phosphine oxides was disclosed by Wang.<sup>15</sup> Given their multifunctional utility, the development of new catalytic systems based on inexpensive metal catalysts for the efficient

synthesis of chiral allylic organophosphorus compounds not only greatly benefits synthetic chemists and pharmacologists, but also represents a significant advance in metal catalysis. The past few decades have witnessed tremendous advances in the nickel catalyst.<sup>16</sup> Apart from low cost and ready availability, the nickel catalyst holds a unique reactivity profile.<sup>17</sup> As a continuation of our previous studies on nickel-catalyzed functionalization of alkenes,<sup>18</sup> particularly the asymmetric hydroamination of 1,3-dienes<sup>19</sup> and inspired by Dong's work,<sup>14</sup> we speculated that the application of a smaller nickel catalyst would allow the hydrophosphinylation reaction to occur

Table 1 Optimization of reaction conditions<sup>a</sup>

Entry	Deviation from standard conditions	Yield (%)	rr (3aa : 4aa + 5aa + 6aa)	ee (%)
1	None	98 <sup>b</sup>	>20 : 1	>99
2	L2 instead of L1	35	>20 : 1	-47
3	L3 instead of L1	6	ND	ND
4	L4 instead of L1	67	>20 : 1	61
5	L5 instead of L1	24	>20 : 1	-68
6	L6 instead of L1	16	>20 : 1	15
7	L7 instead of L1	62	>20 : 1	93
8	L8 instead of L1	31	>20 : 1	36
9	A2 instead of A1	Trace	ND	ND
10	A3 instead of A1	Trace	ND	ND
11	A4 instead of A1	Trace	ND	ND
12	A5 instead of A1	Trace	ND	ND
13	Without A1	NP	—	—
14	Toluene instead of THF	68	>20 : 1	>99
15	EtOAc instead of THF	71	>20 : 1	95
16	DCE instead of THF	6	ND	ND
17	DMF instead of THF	9	ND	ND
18	1,4-Dioxane instead of THF	59	>20 : 1	98
19	MTBE instead of THF	38	>20 : 1	94
20	80 °C	92	>20 : 1	>99
21	50 °C	33	>20 : 1	>99
22	25 °C	Trace	ND	ND

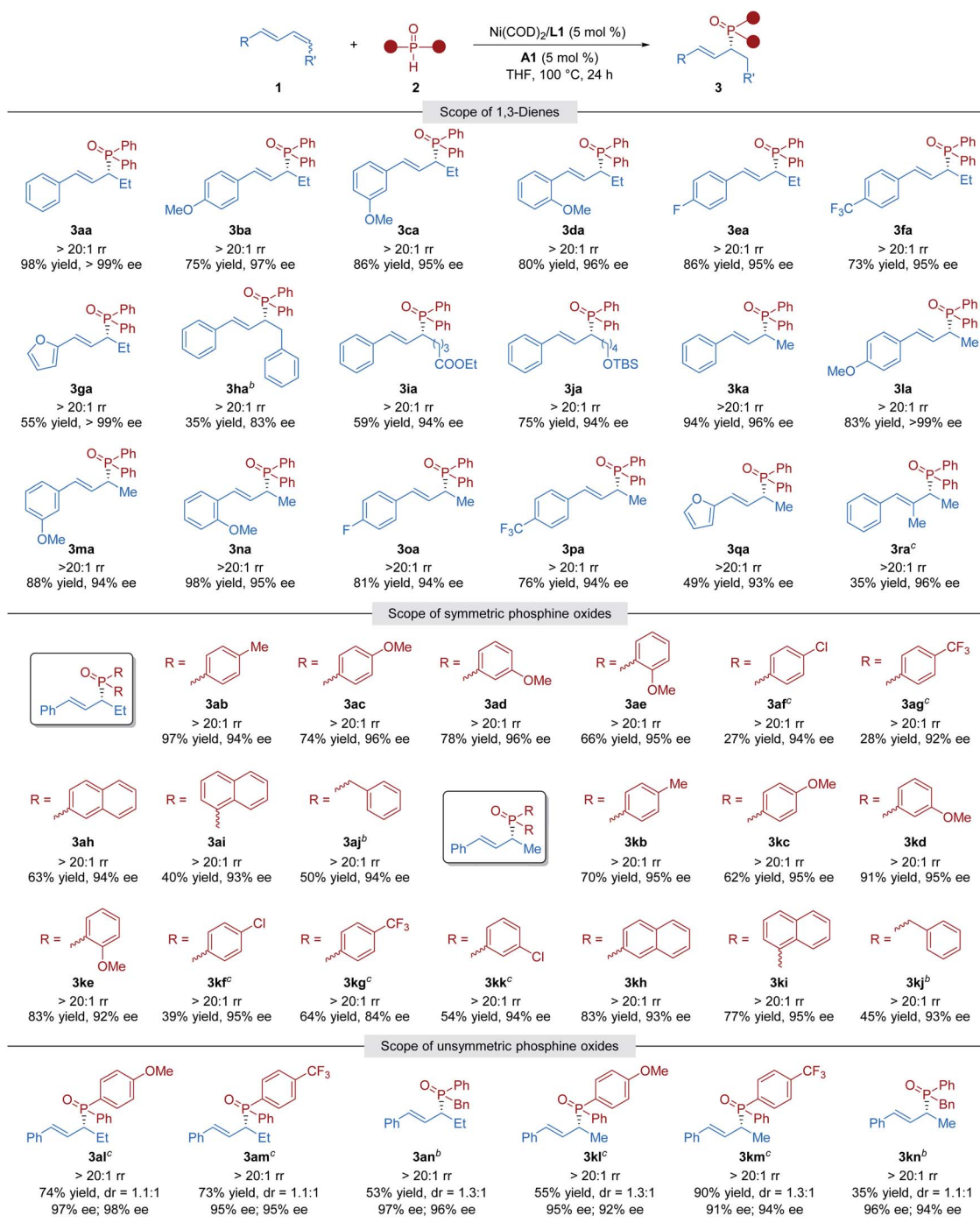


<sup>a</sup> Unless otherwise noted, all reactions were carried out with 0.24 mmol **1a** (*E,Z* : *E,E* = 3.0 : 1), 0.20 mmol **2a**, 5.0 mol% Ni(COD)<sub>2</sub>, 5.0 mol% ligand, and 5.0 mol% acid in 1 mL solvent at 100 °C for 24 h. Yields were determined by gas chromatography analysis, using naphthalene as the internal standard. The rr (regioisomer ratio) was determined by <sup>31</sup>P NMR analysis of the reaction mixture. The ee (enantiomeric excess) values were determined by HPLC analysis using a chiral stationary phase. ND, not determined. NP, no product. <sup>b</sup> Isolated yield.



under milder conditions and has better stereocontrol, leading to the development of a highly enantioselective nickel-catalyzed reaction. Herein we describe our success in the above speculations, resulting in the development of asymmetric nickel/Brønsted acid-catalyzed hydrophosphinylation of 1,3-dienes with secondary phosphine oxides (Fig. 1d). This

methodology tolerates both 1,4-disubstituted acyclic dienes and terminal 1,3-dienes, and is characterized by an inexpensive catalyst and high regio- and enantioselectivity. This study provides an efficient access to a diversity of chiral allylic organophosphorus compounds from readily available starting materials.

Table 2 Substrate scope<sup>a</sup>

<sup>a</sup> See the ESI for details. Data are presented as mean values from two experiments. Isolated yields are reported. The rr was determined by <sup>31</sup>P NMR analysis of the reaction mixture. The dr (diastereomer ratio) was determined by <sup>1</sup>H NMR or <sup>31</sup>P NMR analysis. ee values were determined by HPLC analysis using a chiral stationary phase. <sup>b</sup> 48 h. <sup>c</sup> 80 h.



## Results and discussion

We began our studies by carrying out reactions of the *E,Z/E,E* mixture of 1,4-disubstituted 1,3-diene **1a**<sup>20</sup> with commercially available diphenylphosphine oxide **2a** (Table 1). After careful evaluation of all reaction parameters, we found that a combination of 5 mol% Ni(COD)<sub>2</sub>, 5 mol% (*S*)-BINAP (**L1**), and 5 mol% TsOH·H<sub>2</sub>O (**A1**) in tetrahydrofuran (THF) at 100 °C provided the 1,2-hydrophosphinylation product **3aa** in high yield with excellent enantioselectivity (98% yield and >99% ee, entry 1). The use of plane chiral ligand **L2**, spiro ligand (*R*)-SDP (**L3**), P chiral ligand (*R<sub>C</sub>,S<sub>P</sub>*)-DuanPhos (**L4**), rigid ligand (*S,S*)-Me-DuPhos (**L5**), flexible ligand (*R*)-DIOP (**L6**), (*S,S*)-Ph-BPE (**L7**), or (*S,S*)-BDPP (**L8**) instead of axially chiral biaryl bisphosphorus ligands (*S*)-BINAP (**L1**) provided the 1,2-hydrophosphinylation product **3aa** with either low yield or poor enantioselectivity (entries 2–8). Control experiments indicated that the acid cocatalyst TsOH·H<sub>2</sub>O (**A1**) was essential for the success of this hydrophosphinylation reaction; when switching from TsOH·H<sub>2</sub>O (**A1**) to other Brønsted acids, the reaction was almost inert (entries 9–13). In addition, the choice of the solvent had an obvious effect on the yield, but little effect on the enantioselectivity (entries 14–19). The reaction activity decreased obviously when the temperature was lowered (entries 20–22). Specifically, no other regioisomers (**4aa**, **5aa** or **6aa**) were detected in these reactions (entries 1–22).

With the optimal conditions in hand, we shifted our attention to investigate the generality of this nickel/Brønsted acid-catalyzed asymmetric hydrophosphinylation reaction. Utilizing **2a**, we initially examined the scope of the internal 1,3-dienes. As shown in Table 2, we began with a series of 1-methyl-4-substituted phenyl-1,3-butadiene substrates. Regardless of the electronic properties or the position of the substituent on the benzene ring, all the tested aryl-alkyl-substituted 1,3-dienes could be transformed into the desired chiral allylic phosphine oxides in high yields with excellent regio- and enantioselectivity (**3aa**–**3fa**). 1,3-Dienes with a furan ring substituent also gave the corresponding hydrophosphinylation product (**3ga**) in moderate yield with perfect regio- and enantioselectivity (55% yield, >20 : 1 rr and >99% ee). In particular, symmetric aryl-aryl-substituted 1,3-diene, which is a challenging substrate in transition metal-catalyzed hydrofunctionalizations,<sup>12a</sup> reacted smoothly with diphenylphosphine oxides to give the desired

product **3ha** with >20 : 1 rr and 83% ee, although in low yield. In addition, the substrate bearing an alkyl chain with a terminal ethyl ester (COOEt) or silyl ether (OTBS) group afforded the desired products **3ia** and **3ja** in 59% and 75% yields respectively, both with >20 : 1 rr and 94% ee. We also investigated the hydrophosphinylation of various terminal 1,3-dienes with phosphine oxide **2a**. We found that a variety of aryl-substituted dienes could be transformed into chiral allylic phosphine oxide products **3ka**–**3ra** with moderate to high reactivity (35%–98% yield) and excellent selectivity (>20 : 1 rr, 93–99% ee). Unfortunately, alkyl-alkyl-substituted 1,3-dienes gave the corresponding hydrophosphinylation products with poor regioselectivity (see the ESI† for details).

Subsequently, the scope of secondary phosphine oxides was studied. A set of symmetric secondary phosphine oxides were examined with both internal and terminal dienes under the optimal conditions. As shown in Table 2, this hydrophosphinylation tolerates both aryl and benzyl phosphine oxides, thus produced a series of structurally and electronically different chiral allylic phosphine oxides (**3ab**–**3aj** and **3kb**–**3kk**). Overall, electron-deficient phosphine oxides provided lower yields than electron-rich ones (**3af**, **3ag**, **3kf**, **3kg** and **3kk** vs. **3ac**–**3ae** and **3kc**–**3ke**), probably due to their weaker nucleophilicity. Notably, fused ring motifs, which are the basis of a large class of ligand scaffolds,<sup>21</sup> can also be incorporated in the phosphine oxide partner to generate 1,2-hydrophosphinylation products (**3ah**, **3ai**, **3kh**, and **3ki**). Regrettably, dialkyl phosphine oxides were scarcely tolerated in the transformation (see the ESI† for details). We also studied the dynamic kinetic asymmetric transformation of unsymmetric secondary phosphine oxides under the standard conditions, which could construct vicinal C-stereogenic and P-stereogenic synthons simultaneously. The hydrophosphinylation of 1,4-disubstituted 1,3-diene **1a** with racemic unsymmetric phosphine oxides ( $\pm$ )-**2l**, ( $\pm$ )-**2m**, and ( $\pm$ )-**2n** gave the expected products in moderate to good yield (53–74% yield) with excellent regio- and enantioselectivity (>20 : 1 rr, 95–98% ee), but with no diastereocontrolling (dr = 1.1 : 1–1.3 : 1) (**3al**–**3an**). The similar results were obtained in the transformation of terminal 1,3-diene **1k** with unsymmetric phosphine oxides (**3kl**–**3kn**). To further determine whether the reaction undergoes kinetic resolution or dynamic kinetic resolution,<sup>22</sup> the hydrophosphinylation of model 1,3-diene substrates **1a** and **1k** with an excess of unsymmetric secondary phosphine oxide ( $\pm$ )-**2n** was

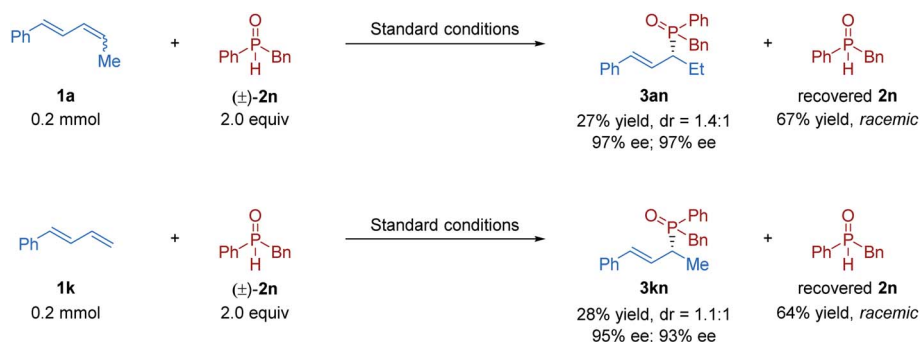


Fig. 2 Kinetic resolution/dynamic kinetic resolution investigations.



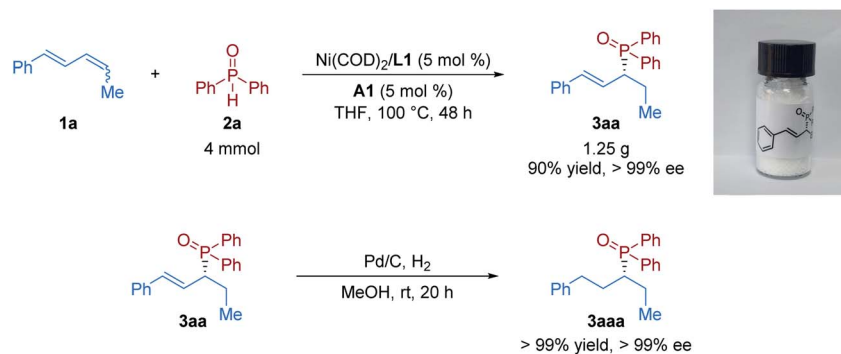
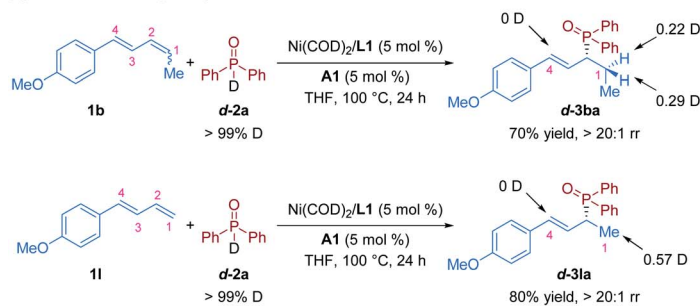


Fig. 3 Scale-up reaction and derivatization of the product.

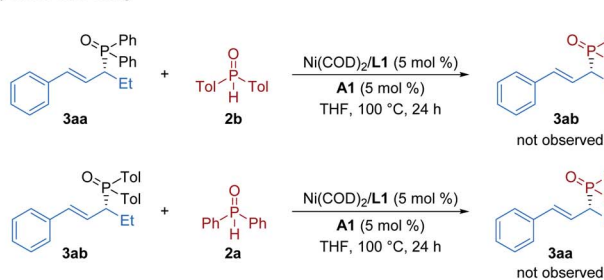
conducted under the standard reaction conditions respectively. The desired chiral allylic phosphine oxide products **3an** and **3kn** were obtained with a diastereomeric ratio close to 1 : 1, and the

recovered **2n** was totally racemic in both cases (Fig. 2). Thus, neither the kinetic resolution nor dynamic kinetic resolution

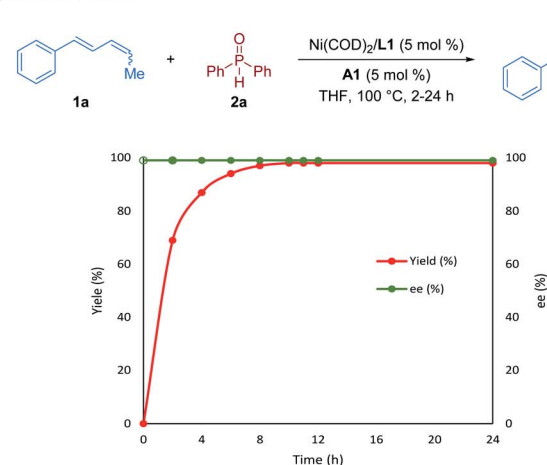
(a) Deuterium-labeling study



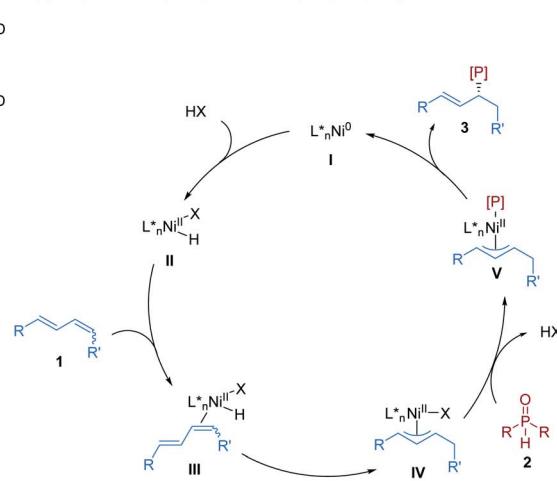
(b) Cross-over study



(c) Reaction profiles



(d) Proposed catalytic cycle for the hydrophosphinylation of 1,3-dienes



(e) Stereochemical model

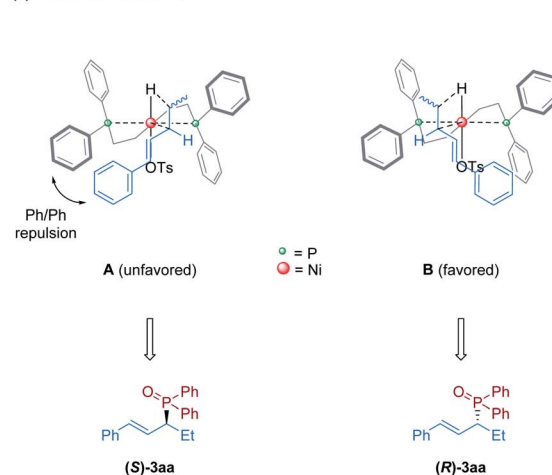


Fig. 4 Mechanistic investigations: (a) deuterium-labeling study; (b) cross-over study; (c) reaction profiles; (d) proposed catalytic cycle for the hydrophosphinylation of 1,3-dienes; (e) stereochemical model.



phenomenon exists in this nickel/Brønsted acid dual-catalyzed hydrophosphinylation.

Furthermore, to demonstrate the practicability of this protocol, a scale-up experiment was performed next. The product **3aa** was obtained in the same level of yield and enantioselectivity (90% yield with >99% ee) from a gram-scale experiment of the model reaction (Fig. 3). The chiral allylic phosphine oxide product could be further manipulated to access various useful functionalities. Then derivatization of the product was conducted. Upon exposure of **3aa** to a H<sub>2</sub> atmosphere with the Pd/C catalyst, the hydrogenation product **3aaa** was obtained in quantitative yield without loss of enantioselectivity.

To obtain further information on this transformation, mechanistic investigations were conducted. First, we performed hydrophosphinylation of internal diene **1b** with deuterium-labeled phosphine oxide **d-2a** under standard reaction conditions, which afforded **d-3ba** with deuterium only at the C1 position; similar results were obtained when the terminal diene **1l** was used (Fig. 4a). These results disclosed that the hydrogen source is from the secondary phosphine oxide, and no reversible 1,4-addition occurs in this nickel-catalyzed hydrophosphinylation, which is inconsistent with the Pd-catalyzed system.<sup>14</sup> To determine if C–P bond formation is a reversible step in this reaction, we conducted the cross-over experiments by subjecting a mixture of **3aa** and **2b** or **3ab** and **2a** to the standard conditions. However, possible crossover products **3ab** and **3aa** were not observed (Fig. 4b). These experiments suggest that this nickel/Brønsted acid-catalyzed hydrophosphinylation reaction is not a reversible transformation. Furthermore, the results of time-course experiments (Fig. 4c) showed that there was no alteration of enantioselectivity during the reaction. This result further indicates that the formation of C–P bonds is irreversible, which is inconsistent with a previous report on the nickel-catalyzed hydroamination reaction.<sup>19</sup>

On the basis of our observations and previous reports,<sup>14,19</sup> we proposed a catalytic cycle for this nickel-catalyzed hydrophosphinylation reaction, as depicted in Fig. 4d. The Ni(0) precatalyst undergoes ligand substitution with (*S*)-BINAP to form chiral monomeric species **I**, and subsequent oxidative addition to TsOH·H<sub>2</sub>O (HX) forms Ni–H species **II**. Then, selective insertion of 1,3-diene **1** provides the key π-allyl nickel intermediate **IV** via species **III**. Species **IV** then undergoes a ligand exchange or nucleophilic attack with secondary phosphine oxide **2** to form species **V**. Finally, species **V** undergoes reductive elimination to furnish allylic phosphine oxide **3** and regenerates the Ni-catalyst **I**. To explore the stereochemical control of the reactions, we proposed a stereochemical model of the transition states of the diene insertion step, as shown in Fig. 4e. Because of Ph/Ph repulsion, model **B** is favored to afford the **R** configuration product.

In this hydrophosphinylation reaction, high enantioselectivity was observed regardless of the *E,Z/E,E* ratio of the starting 1,3-dienes. To explore the origin of the enantioselectivity, we also calculated the energies of the transition states of the diene insertion step for the reaction of (*E,Z*)-**1a** and (*E,E*)-**1a** to afford (*R*)-**3aa** and (*S*)-**3aa**, respectively (see the

ESI† for details). The results suggested that both (*E,Z*)-**1a** and (*E,E*)-**1a** underwent an enantiodetermining step to give (*R*)-**3aa** as the predominant product.

## Conclusions

In summary, we have developed an asymmetric nickel/Brønsted acid-catalyzed hydrophosphinylation reaction of 1,3-dienes with secondary phosphine oxides, featuring highly regio- and enantioselective control with an inexpensive chiral catalyst. This protocol allows the synthesis of a broad range of chiral allylic phosphine oxides in a step and atom-economical fashion from easily accessible materials. Good functional group tolerance and scalability demonstrate the potential of this method in synthesis. Preliminary mechanistic studies indicate that C–P bond formation is an irreversible step. We believe that this chemistry will greatly benefit the biomedical chemistry and chiral ligand development.

## Data availability

The data that support the findings of this study are available within the article and its ESI files.†

## Author contributions

J. Long and Y. Li performed the experiments, collected and analyzed the data. W. Zhao and G. Yin conceived and directed the project. J. Long and G. Yin wrote the manuscript.

## Conflicts of interest

There are no conflicts to declare.

## Acknowledgements

This work was supported by the National Natural Science Foundation of China (21871211 and 22122107), the Fundamental Research Funds for Central Universities (2042019kf0208), and China Postdoctoral Science Foundation (2021M702519). We thank Prof. Qingquan Lu at Wuhan University for sharing the basic instruments. We thank Dr Austin Schultz, from Liwen Bianji (www.liwenbianji.cn/), for editing the language of the draft of this manuscript. The numerical calculations in this paper have been done on the supercomputing system in the Supercomputing Centre of Wuhan University.

## Notes and references

- (a) *Phosphorus chemistry I asymmetric synthesis and bioactive compounds*, Topics in current chemistry 360, ed. J.-L. Montchamp, Springer, Switzerland, 2015; (b) M. Dutartre, J. Bayardon and S. Jugé, *Chem. Soc. Rev.*, 2016, **45**, 5771–5794.
- (a) P. W. N. M. van Leeuwen, P. C. J. Kamer, J. N. H. Reek and P. Dierkes, *Chem. Rev.*, 2000, **100**, 2741–2769; (b) W. Tang and X. Zhang, *Chem. Rev.*, 2003, **103**, 3029–3069; (c) X. Cui



- and K. Burgess, *Chem. Rev.*, 2005, **105**, 3272–3296; (d) T. Imamoto, *J. Synth. Org. Chem., Jpn.*, 2007, **65**, 1060–1069; (e) P. W. N. M. van Leeuwen, P. C. J. Kamer, C. Claver, O. Pàmies and M. Diéguez, *Chem. Rev.*, 2011, **111**, 2077–2118; (f) Y.-M. He, Y. Feng and Q.-H. Fan, *Acc. Chem. Res.*, 2014, **47**, 2894–2906; (g) W. Zhao, D. Yang and Y. Zhang, *Chin. J. Org. Chem.*, 2016, **36**, 2301–2316; (h) G. Xu, C. H. Senanayake and W. Tang, *Acc. Chem. Res.*, 2019, **52**, 1101–1112; (i) F. Wan and W. Tang, *Chin. J. Chem.*, 2021, **39**, 954–968.
- 3 (a) J. L. Methot and W. R. Roush, *Adv. Synth. Catal.*, 2004, **346**, 1035–1050; (b) J. Seayad and B. List, *Org. Biomol. Chem.*, 2005, **3**, 719–724; (c) S. J. Connon, *Angew. Chem., Int. Ed.*, 2006, **45**, 3909–3912; (d) M. Benaglia and S. Rossi, *Org. Biomol. Chem.*, 2010, **8**, 3824–3830; (e) Y. Wei and M. Shi, *Acc. Chem. Res.*, 2010, **43**, 1005–1018; (f) H. Ni, W.-L. Chan and Y. Lu, *Chem. Rev.*, 2018, **118**, 9344–9411; (g) R. Xu, H. Yang and W. Tang, *Chin. J. Org. Chem.*, 2020, **40**, 1409–1422.
- 4 E. E. Coyle, B. J. Doonan, A. J. Holohan, K. A. Walsh, F. Lavigne, E. H. Krenske and C. J. O'Brien, *Angew. Chem., Int. Ed.*, 2014, **53**, 12907–12911.
- 5 (a) J. M. Gil, J. H. Hah, K. Y. Park and D. Y. Oh, *Synth. Commun.*, 2000, **30**, 789–794; (b) S. Demay, M. Lotz, K. Polborn and P. Knochel, *Tetrahedron: Asymmetry*, 2001, **12**, 909–914; (c) M. Stankevic, M. Jaklinska and K. M. Pietrusiewicz, *J. Org. Chem.*, 2012, **77**, 1991–2000; (d) M. Jaklinska, M. Cordier and M. Stankevic, *J. Org. Chem.*, 2016, **81**, 1378–1390.
- 6 (a) N. J. S. Harmat and S. Warren, *Tetrahedron Lett.*, 1990, **31**, 2743–2746; (b) P. Camps, G. Colet, M. Font-Bardia, V. Muñoz-Torrero, X. Solansb and S. Vázquez, *Tetrahedron*, 2002, **58**, 3473–3484; (c) P. Camps, G. Colet, M. Font-Bardia, V. Muñoz-Torrero, X. Solansb and S. Vázquez, *Tetrahedron: Asymmetry*, 2002, **13**, 759–778; (d) J. H. Hah, B. S. Lee, S. Y. Lee and H.-Y. Lee, *Tetrahedron Lett.*, 2003, **44**, 5811–5814.
- 7 (a) T. Nishimura, S. Hirabayashi, Y. Yasuhara and T. Hayashi, *J. Am. Chem. Soc.*, 2006, **128**, 2556–2557; (b) P. Butti, R. Rochat, A. D. Sadow and A. Togni, *Angew. Chem., Int. Ed.*, 2008, **47**, 4878–4881; (c) T. Nishimura, X.-X. Guo and T. Hayashi, *Chem.-Asian J.*, 2008, **3**, 1505–1510; (d) T. Kawamoto, S. Hirabayashi, X.-X. Guo, T. Nishimura and T. Hayashi, *Chem. Commun.*, 2009, 3528–3530; (e) L. Hong, W. Sun, C. Liu, D. Zhao and R. Wang, *Chem. Commun.*, 2010, **46**, 2856–2858; (f) Y. Huang, R. J. Chew, S. A. Pullarkat, Y. Li and P. H. Leung, *J. Org. Chem.*, 2012, **77**, 6849–6854; (g) M. Hatano, T. Horibe and K. Ishihara, *Angew. Chem., Int. Ed.*, 2013, **52**, 4549–4553; (h) X.-Y. Yang, W. S. Tay, Y. Li, S. A. Pullarkat and P.-H. Leung, *Organometallics*, 2015, **34**, 5196–5201; (i) W. Hu, E.-Q. Li, Z. Duan and F. Mathey, *J. Org. Chem.*, 2020, **85**, 14772–14778.
- 8 (a) X.-T. Liu, Y.-Q. Zhang, X.-Y. Han, S.-P. Sun and Q.-W. Zhang, *J. Am. Chem. Soc.*, 2019, **141**, 16584–16589; (b) H. Qiu, Q. Dai, J. He, W. Li and J. Zhang, *Chem. Sci.*, 2020, **11**, 9983–9988; (c) S. Zhang, J.-Z. Xiao, Y.-B. Li, C.-Y. Shi and L. Yin, *J. Am. Chem. Soc.*, 2021, **143**, 9912–9921.
- 9 (a) N. J. Adamson, K. C. E. Wilbur and S. J. Malcolmson, *J. Am. Chem. Soc.*, 2018, **140**, 2761–2764; (b) L. Cheng, M.-M. Li, L.-J. Xiao, J.-H. Xie and Q.-L. Zhou, *J. Am. Chem. Soc.*, 2018, **140**, 11627–11630; (c) L. Cheng, M.-M. Li, B. Wang, L.-J. Xiao, J.-H. Xie and Q.-L. Zhou, *Chem. Sci.*, 2019, **10**, 10417–10421; (d) L. Lv, D. Zhu, Z. Qiu, J. Li and C.-J. Li, *ACS Catal.*, 2019, **9**, 9199–9205; (e) S. Park, N. J. Adamson and S. J. Malcolmson, *Chem. Sci.*, 2019, **10**, 5176–5182.
- 10 (a) O. Löber, M. Kawatsura and J. F. Hartwig, *J. Am. Chem. Soc.*, 2001, **123**, 4366–4367; (b) N. J. Adamson, E. Hull and S. J. Malcolmson, *J. Am. Chem. Soc.*, 2017, **139**, 7180–7183; (c) X.-H. Yang and V. M. Dong, *J. Am. Chem. Soc.*, 2017, **139**, 1774–1777; (d) S. Park and S. J. Malcolmson, *ACS Catal.*, 2018, **8**, 8468–8476; (e) G. Tran, W. Shao and C. Mazet, *J. Am. Chem. Soc.*, 2019, **141**, 14814–14822.
- 11 (a) X.-H. Yang, R. T. Davison and V. M. Dong, *J. Am. Chem. Soc.*, 2018, **140**, 10443–10446; (b) X.-H. Yang, R. T. Davison, S.-Z. Nie, F. A. Cruz, T. M. McGinnis and V. M. Dong, *J. Am. Chem. Soc.*, 2019, **141**, 3006–3013; (c) Q. Zhang, D. Dong and W. Zi, *J. Am. Chem. Soc.*, 2020, **142**, 15860–15869; (d) M.-M. Li, L. Cheng, L.-J. Xiao, J.-H. Xie and Q.-L. Zhou, *Angew. Chem., Int. Ed.*, 2021, **60**, 2948–2951.
- 12 (a) N. J. Adamson and S. J. Malcolmson, *ACS Catal.*, 2019, **10**, 1060–1076; (b) R. Blicke, M. Taillefer and F. Monnier, *Chem. Rev.*, 2020, **120**, 13545–13598; (c) G. Li, X. Huo, X. Jiang and W. Zhang, *Chem. Soc. Rev.*, 2020, **49**, 2060–2118.
- 13 (a) L.-B. Han, N. Choi and M. Tanaka, *Organometallics*, 1996, **15**, 3259–3261; (b) F. Mirzaei, L.-B. Han and M. Tanaka, *Tetrahedron Lett.*, 2001, **42**, 297–299; (c) L.-B. Han and C.-Q. Zhao, *J. Org. Chem.*, 2005, **70**, 10121–10123; (d) D. Zhao and R. Wang, *Chem. Soc. Rev.*, 2012, **41**, 2095–2108; (e) S. Pullarkat, *Synthesis*, 2015, **48**, 493–503; (f) Z.-W. Lu, H. Zhang, Z. Yang, N. Ding, L. Meng and J. Wang, *ACS Catal.*, 2019, **9**, 1457–1463; (g) Q. Dai, L. Liu, Y. Qian, W. Li and J. Zhang, *Angew. Chem., Int. Ed.*, 2020, **59**, 20645–20650; (h) Z. Yang, X. Gu, L.-B. Han and J. Wang, *Chem. Sci.*, 2020, **11**, 7451–7455.
- 14 S.-Z. Nie, R. T. Davison and V. M. Dong, *J. Am. Chem. Soc.*, 2018, **140**, 16450–16454.
- 15 Z. Yang and J. Wang, *Angew. Chem., Int. Ed.*, 2021, **60**, 27288–27292.
- 16 (a) H. Zhang, Q. Gu and S. You, *Chin. J. Org. Chem.*, 2019, **39**, 15–27; (b) A. L. Clevenger, R. M. Stolley, J. Aderibigbe and J. Louie, *Chem. Rev.*, 2020, **120**, 6124–6196; (c) H. Dai, F. Wu and D. Bai, *Chin. J. Org. Chem.*, 2020, **40**, 1423–1436; (d) Y. Liu, X.-Q. Dong and X. Zhang, *Chin. J. Org. Chem.*, 2020, **40**, 1096–1104; (e) A. D. Marchese, T. Adrianov and M. Lautens, *Angew. Chem., Int. Ed.*, 2021, **60**, 16750–16762; (f) C. Zhu, H. Yue, J. Jia and M. Rueping, *Angew. Chem., Int. Ed.*, 2021, **60**, 17810–17831.
- 17 (a) S. Z. Tasker, E. A. Standley and T. F. Jamison, *Nature*, 2014, **509**, 299–309; (b) V. P. Ananikov, *ACS Catal.*, 2015, **5**, 1964–1971; (c) B. Su, Z.-C. Cao and Z.-J. Shi, *Acc. Chem. Res.*, 2015, **48**, 886–896; (d) S. Manna, K. K. Das, S. Nandy, D. Aich, S. Paul and S. Panda, *Coord. Chem. Rev.*, 2021, **448**, 214165.



- 18 (a) Y. Li, H. Pang, D. Wu, Z. Li, W. Wang, H. Wei, Y. Fu and G. Yin, *Angew. Chem., Int. Ed.*, 2019, **58**, 8872–8876; (b) W. Wang, C. Ding, Y. Li, Z. Li, Y. Li, L. Peng and G. Yin, *Angew. Chem., Int. Ed.*, 2019, **58**, 4612–4616; (c) Y. Li, H. Wei, D. Wu, Z. Li, W. Wang and G. Yin, *ACS Catal.*, 2020, **10**, 4888–4894; (d) W. Wang, C. Ding and G. Yin, *Nat. Catal.*, 2020, **3**, 951–958; (e) Z. Li, D. Wu, C. Ding and G. Yin, *CCS Chem.*, 2021, **3**, 576–582; (f) B. Zhao, Y. Li, H. Li, M. Belal, L. Zhu and G. Yin, *Sci. Bull.*, 2021, **66**, 570–577; (g) C. Ding, Y. Ren, C. Sun, J. Long and G. Yin, *J. Am. Chem. Soc.*, 2021, **143**, 20027–20034; (h) M. Belal, Z. Li, L. Zhu and G. Yin, *Sci. China: Chem.*, 2021, DOI: 10.1007/s11426-021-1172-x; (i) H. Li, J. Long, Y. Li, W. Wang, H. Pang and G. Yin, *Eur. J. Org. Chem.*, 2021, **2021**, 1424–1428.
- 19 J. Long, P. Wang, W. Wang, Y. Li and G. Yin, *iScience*, 2019, **22**, 369–379.
- 20 The substrate was inert in our previous nickel-catalyzed asymmetric hydroamination: ref. 19.
- 21 (a) Q. Wang, Q. Gu and S.-L. You, *Acta Chim. Sin.*, 2019, **77**, 690–704; (b) C. Claver, E. Fernandez, A. Gillon, K. Heslop, D. J. Hyett, A. Martorell, A. G. Orpen and P. G. Pringle, *Chem. Commun.*, 2000, 961–962; (c) C. Li and S. Yang, *Chin. J. Org. Chem.*, 2020, **40**, 2159–2160.
- 22 (a) Q. Dai, W. Li, Z. Li and J. Zhang, *J. Am. Chem. Soc.*, 2019, **141**, 20556–20564; (b) Q. Dai, L. Liu and J. Zhang, *Angew. Chem., Int. Ed.*, 2021, **60**, 27247–27252.

